Energy 52 (2013) 265–278

Contents lists available at SciVerse ScienceDirect

Energy

journal homepage: www.elsevier.com/locate/energy

Energetic analysis of a system integrated with biomass gasification

Janusz Kotowicz [a], Aleksander Sobolewski [b], Tomasz Iluk [b], *

[a] Institute of Power Engineering and Turbomachinery, Silesian University of Technology, Konarskiego 18, 44-100 Gliwice, Poland
[b] Institute for Chemical Processing of Coal, Zamkowa 1, 41-803 Zabrze, Poland

ARTICLE INFO

Article history:
Received 30 July 2012
Received in revised form
18 February 2013
Accepted 20 February 2013
Available online 19 March 2013

Keywords:
Biomass
Gasification
Research installation
Piston engine
Efficiency of electricity and heat generation

ABSTRACT

This article presents biomass gasification technology as a possible method for reducing CO_2 emissions in industrial energy generation. The research uses process gas obtained from biomass gasification to fuel a piston-feeding SG (combustion engine). An innovative GG (gas generator) was constructed with a fixed bed, producing approximately 60 kW_t of power, which was tested at The Institute For Chemical Processing Of Coal in Zabrze (Poland). This work demonstrates how the generator parameters influence the accumulation of the contained gas; the pilot construction was characterized based on its ability to generate electrical energy. The installation consists of a fuel-measuring system, a GG, a dry IOG (gas purification system), a current-generating unit and a combustion chamber. The paper describes the dry IOG and its ability to reduce ash and organic impurities and introduces an intermediate demarcation of the process gas stream. The mass and energy balance of the GG is detailed and analyzed with a parametric system for an installation with a power of 1.5 MW_t that uses co-generation to produce both electricity and heat. During gas combustion in a two-stroke piston engine, this system produced approximately 15 kW of electrical energy. The influence of particular fixtures of the system on the efficiency of the entire installation is also covered.

© 2013 Elsevier Ltd. All rights reserved.

1. Introduction

In the near future, the generation of electricity and heat will utilize methods to reduce the environment impact of industrial energy generation. One interesting direction that could facilitate the desirable ecological effects is RES (Renewable Energy Sources), particularly including biomass. The chemical energy in biomass can be converted to usable energy using combustion technology [1,2], co-combustion with coal [3,4] or gasification [5,6]. Gasification is a promising technology for biomass-derived energy due to the specific properties of biomass and its availability [7,8]. Gasification occurs in GGs (gas generators) or reactors. These devices can be divided into general categories: fixed-bed gasifiers [9–11], fluidized-bed gasifiers [12–14] and entrained-flow gasifiers. Fixed-bed reactor technology (and fluidized-bed reactor technology, to a certain degree) has been specifically developed to handle biomass, while entrained-flow gasifiers are mainly used in coal gasification technology, which is characterized by high power outputs [15].

Converting the chemical energy contained in biomass to combustible gas energy significantly increases the feasibility of using biomass to supply energy to small district heating boilers or large boilers [16–18], to produce fuels [19–22] such as methanol [23] or to use in SGs (combustion engines) [8] and gas turbines [24]. The use of process gas to fuel distributed small- and medium-sized co-generation systems that produce electricity and heat contributes to the achievement of the desired minimum value of RES in the overall balance of fuel mix. Biomass gasification technologies are being developed worldwide, including the integration of installations with biomass torrefying units [25]. Additionally, these systems allow the use of local fuel sources [26], thereby eliminating costly transportation. An important feature of biomass gasification technology systems is the ability to use fuel that would otherwise be classified as post-production waste (e.g., from the wood or food industries).

Biomass gasification technology together with high-performance zero-emission installations [27] may help to decrease the amount of CO_2 introduced to the atmosphere.

2. Description of the GG

Our research at The Institute For Chemical Processing Of Coal in Zabrze (Poland) has developed an innovative design for a fixed-bed GG that is part of a biomass gasification installation that generates electricity and heat.

A vital component of the installation is the latest type of biomass GG (patent number PL208616). Fig. 1 shows a schematic of the GG

---

* Corresponding author. Tel.: +48 32 71 00 41; fax: +48 32 271 08 09.
E-mail addresses: tiluk@ichpw.zabrze.pl, janusz.kotowicz@polsl.pl (T. Iluk).

0360-5442/$ – see front matter © 2013 Elsevier Ltd. All rights reserved.
http://dx.doi.org/10.1016/j.energy.2013.02.048

Nomenclature

A	ash
$\dot{m}$	mass flow rate, kg/h
h	specific enthalpy, kJ/kg
H	high, mm
i	contribution
LHV	lower heating value, kJ/kg
M	particle mass, kg/kmol
N	power, kW
$\dot{Q}$	heat flux, kW
t	temperature, °C
u	coefficient
w	coefficient
α	coefficient of the distribution of gas, –
δ	error margin, %
η	efficiency, %
ρ	density, kg/dm^3

Indices

BCHP	biomass combined heat and power
el	electric
f	fuel
GG	gasifier
h	heat
i	component
ICH	gas-cooling installation
in	input (entering)
IOG	gas drying installation
KM	mixing chamber
out	output
r	reactor
s	dry
SG	gas engine
t	thermal
Σ	sum

along with the ascending internal fixtures located within the processing zones. The tested generator consists of a vertical cylindrical reactor with an internal circumference of 400 mm and a height of approximately 900 mm [28,29].

The literature contains a number of examples of GG designs, specifically reactor designs in which air is used as the gasifying agent, while the feed (biomass) is transported through a gravitationally moved bed (fixed bed). These solutions can handle varying levels of solid particle contamination in process gas as well as tars created during biomass thermal processing.

When a system only generates heat from process gas, it does not have to possess low content of ash and tar contaminants. This type of generator may have a simple construction, and the resulting gas may possess high levels of contamination (level of 10,000 mg/m^3 for ash and tar). There are a number of gasification reactor designs, both Polish and international. One example is the EKOD biomass gasification reactor, which is a type of counter-current reactor [30] that comprises two parts: one cylindrical and one conical. The gasification chamber is located in the cylindrical section, while the gasifying agent is introduced via a system of nozzles fitted in the conical part of the reactor. The gas produced is directed to the upper part of the apparatus, where it is subsequently combusted in the boiler. One example in the literature [31] details a reactor that generates heat directly in the GG. The apparatus is cylindrical, generating gas at the bottom and combusting the resulting gas at the top. The gasifying agent is introduced via inlets in the lower part and bottom of the reactor. However, gasification technologies that produce electricity are extremely attractive from a commercial standpoint. Technologically advanced reactor designs have been implemented in a number of countries worldwide, including the Czech Republic [32], China [33,34], Italy and the USA. However, the process gas in these designs is characterized by a high ash particle (concurrent reactor – of IMBERT type) or tar content (counter-current reactor) [33].

The gas must be thoroughly cleaned when used for generating electrical energy by piston engines. Cleaning the gas to levels required by engine producers is difficult, even with a 90% efficient gas cleaning system. Thus, the key problem becomes designing a generator that produces gas with the lowest possible tar content. Low tar content permits effective dust removal via conventional methods, as well as cost-effective residual tar removal to industrially acceptable levels – an essential characteristic for bringing new technology into the scattered power industry. The essence of the ICHPW design is to remove process gas directly from the hot zone of the reactor using a central pipe fitted in the vertical axis, this allows thermal cracking of larger hydrocarbons (tars from

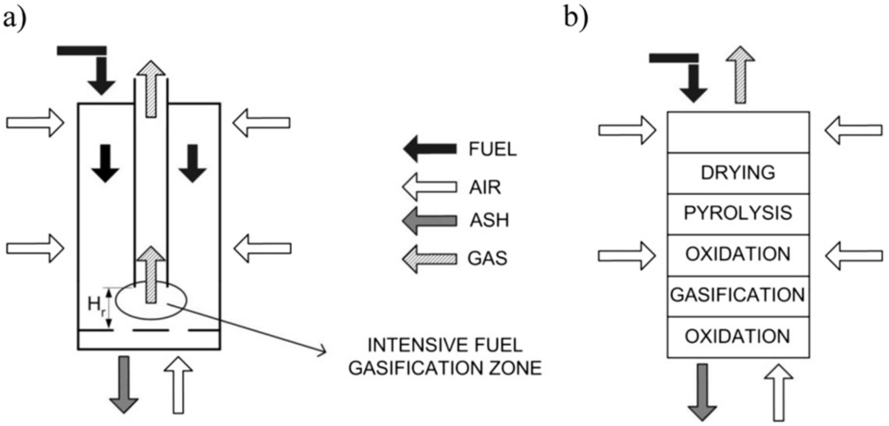

Fig. 1. The gas generator: (a) Technological scheme of the design, (b) Process zones.

biomass pyrolysis) during their flow through the gasification hot zone. We achieved higher temperature gas with several times lower tar content compared to that produced by the counter-current reactor. Furthermore contradictory to the concurrent reactor created process gas has a much lower solid particle content entrained from the lower oxidation zone and reduces partial process gas combustion. Moreover, selecting the appropriate height, H_r (distance between air distributor and inlet to the central pipe) (Fig. 1), for the given apparatus geometry and type of fuel (physicochemical properties of biomass) produces gas with the maximum heating value and the optimal composition. The new generator also has the advantage that the gasifying agent is fed in three different places in the apparatus: underneath the grate, in the middle part and at the top of the fuel bed. Each stream can be separately controlled, which allows control of the size of individual zones based on localized temperature changes. This control is particularly important for optimizing gas production based on the physicochemical parameters of the type of fuel used (such as moisture content and chemical composition).

Moist fuel (Fig. 2) is fed into the upper part of the reactor using a screw conveyor and travels downward in the apparatus. This fuel is then subjected to the following thermal processes: drying, pyrolysis, combustion and gasification. Fuel and air travel concurrently in the drying and pyrolysis zones; a mixed current exists in the gasification zone, while combustion is conducted in a counter-current zone.

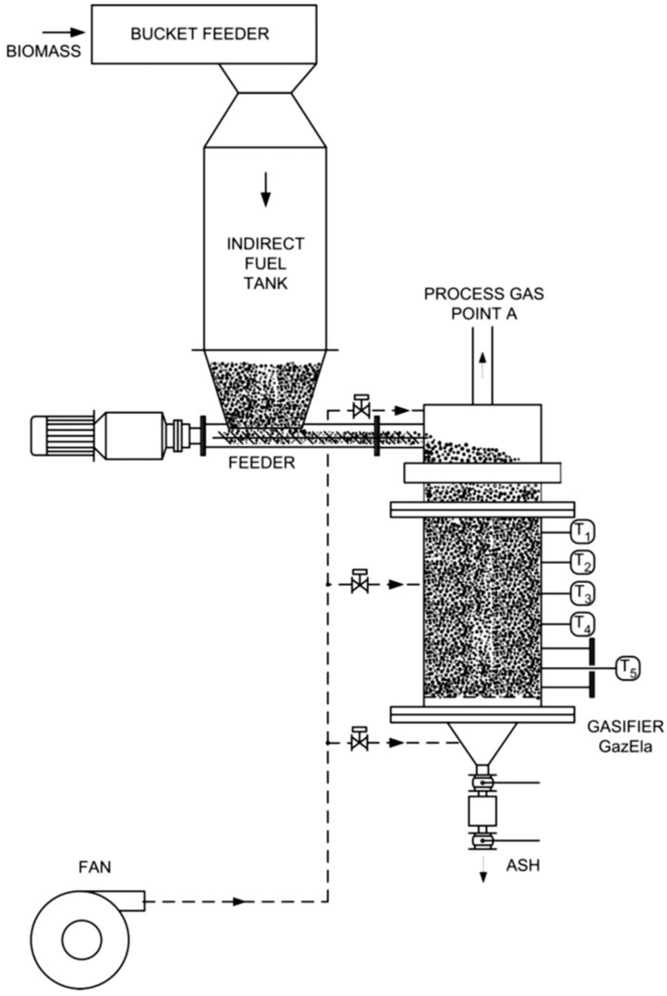

Fig. 2. The gas generator with the fuel-feeding fixture and the process air.

Moisture-containing biomass fed into the reactor in the first step is dried and is transported into the pyrolysis zone with a small amount of top process air. The stream of water vapor created while drying the biomass is passed from the drying zone through the pyrolysis zone (without chemical reaction) to the gasification zone. Here, part of the water vapor stream reacts with hot char, creating hydrogen. The unreacted steam passes to the process gas as a ballast.

Char and tars created during the pyrolysis process are passed to the gasification zone, where part of the products from pyrolysis is combusted in the place where the middle gasifying agent is introduced.

Unreacted char is combusted at the bottom part of the reactor, where the main process air is introduced, providing a heat source for the endothermic gasification reactions. A stream of ash is bled at the bottom part of the reactor by combusting the char produced from the biomass.

The final composition of the process gas is made up of gas from gasification, pyrolytic gas and flue gas created in the combustion process, as well as the portion of the water vapor that was separated while drying the fuel.

Temperature measurements for the individual zones are marked in Fig. 2, while the composition of the produced gas was measured at the generator outlet.

The tested generator yields approximately 60 kW$_t$ (calculated for chemical enthalpy of fed biomass). The apparatus combines the advantages of both the counter-current and concurrent reactors, allowing the use of fuel with different granulation and higher moisture contents [35]. Removing process gas directly from the gasification zone (i.e., high-temperature zone) causes thermolysis of tars and could greatly reduce the amount of highly aromatized substances. Fig. 3 shows pictures of the reactor. At left is the overall view of the reactor; at right is the top of the reactor, with two-level sensors, and in the bottom right corner is the measurement and control system for the upper process air. Fig. 4 shows the bottom part of the reactor with the ash removal system.

3. Description of the biomass gasification installation

The outline of the entire installation for biomass gasification and electricity generation is shown in Fig. 5. The installation consists of a fuel-feeding system and a GG (see Fig. 2), a dry-IOG, a two-stroke piston engine, a combustion chamber and a control system, which allows the specific fixtures to be controlled and the current parameters of the work installation to be observed.

The technological installation process occurs in the following manner: biomass supplies from the fuel stores outside of the technological collection point are transported to the intermediate fuel collection point using a bucket conveyor. The fuel flows from the tank with the assistance of a variable efficiency worm-feeder that is proportional to the GG. The level of fuel within the reactor is maintained automatically by a system with two signaling sensors, producing either a minimal or maximum level of biomass in the equipment under research. After a minimal level of fuel is achieved in the reactor, the worm-feeder automatically starts up to transport the fuel from the collection point and continues until the generator reaches the maximum level of biomass.

In the experimental installation, a gasification agent is used for the atmospheric air, which, when surrounded by low pressure or overpressure, is directed to the reactor with the assistance of a radial fan. The air is introduced into the system at three locations via regulating valves. The gas generated in the reactor is transported to the inertial dust-collector to collect the excess moisture from the process gas (particularly during the start-up process of the installation), as well as the majority of the ash impurities in the gas.

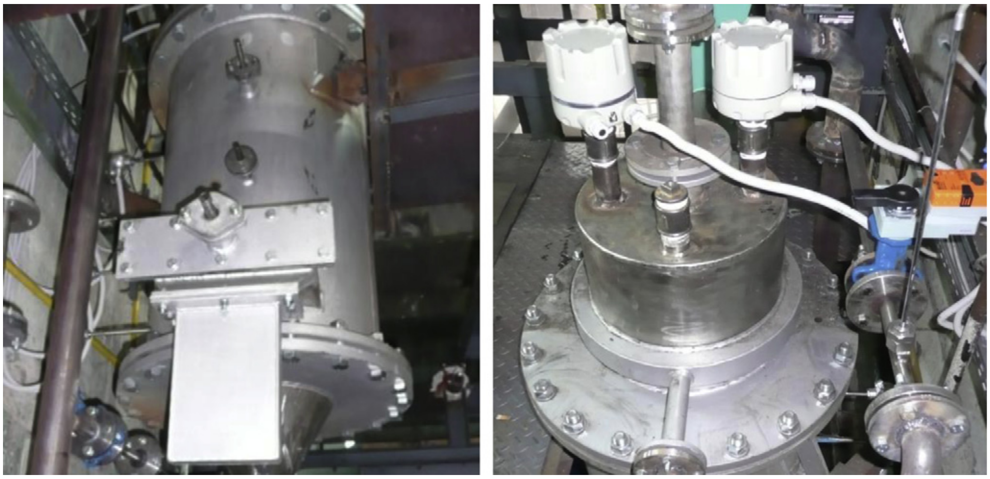

Fig. 3. The GazEla generator – a view of the left and upper parts of the reactor.

The device is a vertical cylindrical tank with a cross-sectional area much greater than that of the central pipe. A vertical plate is installed in the expander's axis to inertially separate the larger ash particles. This process reduces the gas velocity in the dust-collector, allowing heavier pollutant particles to fall onto the system bed, where they are directed to the ash tank by the specified ash-collection system. The inertial expander installed on the process gas pipeline eliminates the effect of the process gas pipeline cross-sectional contraction; such an effect often leads to disturbances in the work of the installation. Initially, the purified gas is transported to the cyclone dust-collector to remove the tiny ash impurities. Next, the gas is directed to the two-level gas cooler. The gas is cooled to a temperature of approximately 30–40 °C in the counter-current heat exchanger to condense any organic impurities or water vapor contained in the gas. The condensed moisture and organic impurities are gathered in the lower heat exchanger collector and are periodically released to a condenser tank directly under the heat exchanger. In the next stage of purification, the gas flows to the adsorber and the two-filter piston fixture. The filled adsorber produces a rinsed coke with a granulation of 10–20 mm.

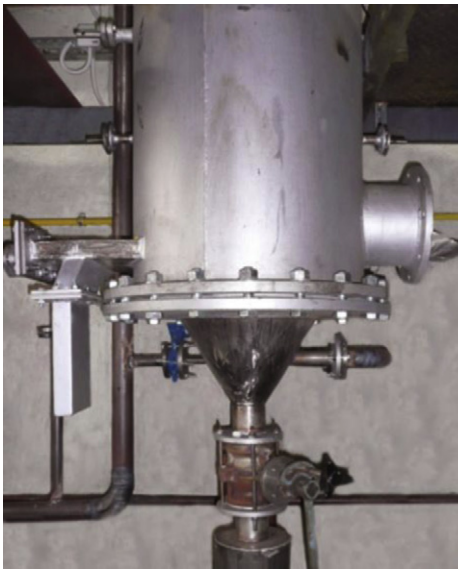

Fig. 4. The GazEla generator – a view of the front part of the reactor.

The two cloth filters are used to remove the finest ash particles and a small part of the organic contaminants. Commercial vehicle filters proper for this type of engine have been used. In this set-up, one filter works while the other is a spare; the filters switch when the pressure drop before and after the appliance increases; that element is removed and is replaced with a new one. The purified combusted gas is then fed to the two-stroke engine or the combustion chamber, and the remaining fumes are emitted through the chimney into the atmosphere.

A two-stroke piston engine with compression ignition was used to generate electric energy using diesel fuel. Table 1 presents the basic parameters of the SG.

In a start-up phase of the current-generating unit, diesel oil was pumped to the piston engine. After the phase of GG and gas cleaning unit start-up, a valve is opened, and the total process gas stream is directed into the engine. In an instant, a decrease in diesel oil consumption by the engine is noticed. The amount of electric power generated by the current-generating unit is controlled by setting the heating power on an electric air heating coil. Total amount of electric energy produced in a research installation is used to supply the electric air heating coil. Such a heating unit is composed of a heating coil and a radial fan, the latter of which is supposed to cool down the heater.

Research continued after the temperatures were stabilized in the inner reactor and in other designated locations of the installation.

The following parameters were constantly monitored during the data collection process:

- The internal temperature of the reactor and the temperature of the gas at the outlet from the reactor, in addition to monitoring specific areas inside the GG (marked as $T_1 \div T_5$ in Fig. 2),
- The accumulation of the generated process gas using a mobile analyzer terminal,
- The measurement of controlled pressure in both the internal reactor and in all outflow apparatus in the system installation,
- The air streams directed to particular zones of the reactor.

Similarly, there was a periodic collection of the following data:

- Fuel moisture content (%),
- The amount of ash impurities,
- The amount of organic impurities,
- Detailed process gas composition,
- The composition of the condensate from process gas cooling.

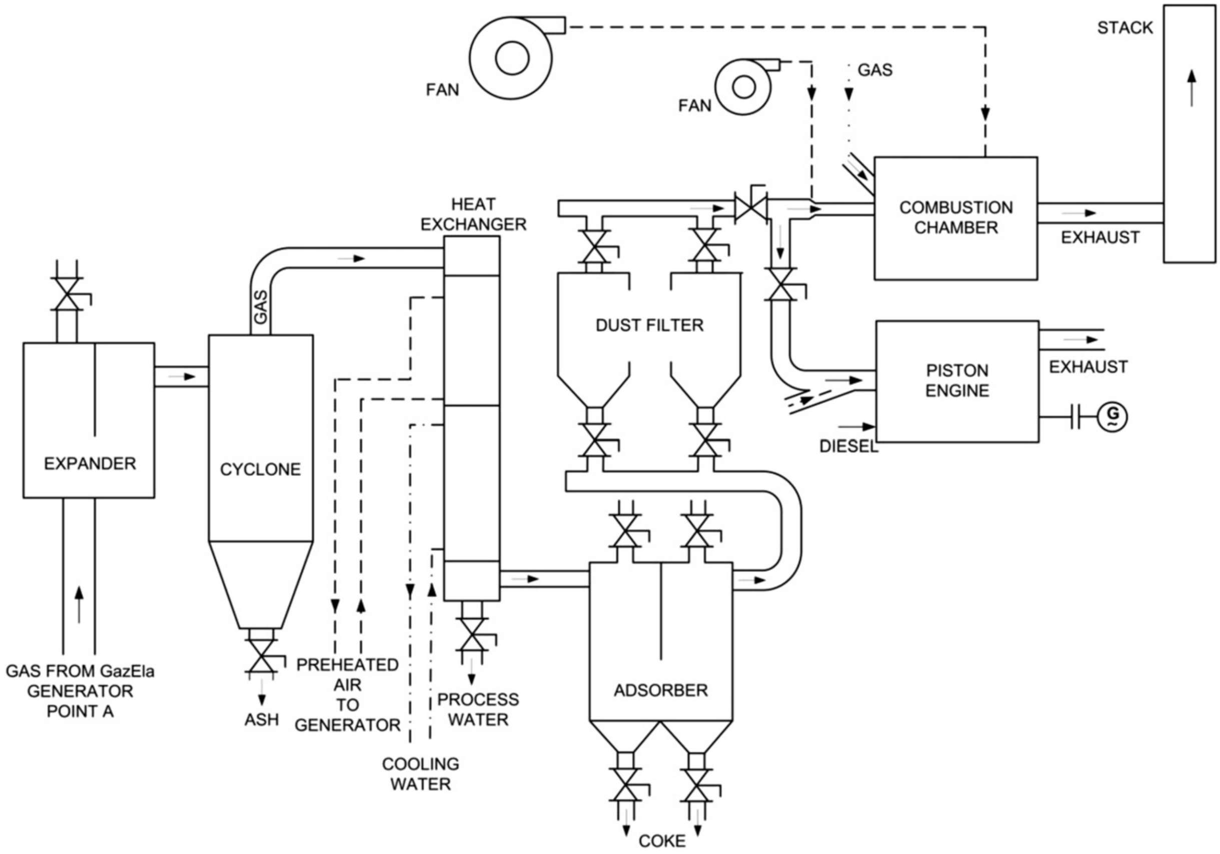

Fig. 5. Outline of the biomass gasification installation for generating electricity.

The basic components of the gas (i.e., CO, CO_2, CH_4, H_2 and O_2) were measured using mobile analytic gas terminals. Samples of the process gas together with basic hydrocarbons and VOCs (volatile organic compounds) (as noted in the Laboratory Of Industrial Gases And Carbon-Based Products, IChPW, which operates under quality control systems consistent with norm PN-EN ISO/IEC 17025:2005 confirmed with certificate Nr. AB 081 (by PCA)) were measured by chromatographic analysis. The organic and ash impurities were collected by a system consisting of an electrically heated sounder, two washers, a set of resin-filled XAD-2 tubes, an active coal-gas counter and a vacuum pump.

4. Research results

The biomass fragments used in the research included wood slivers (Fig. 6). Table 2 presents the physical and chemical characteristics of the biomass.

Fig. 7 shows the changes over time in the main process gas components during the gasification of alder chips. The figure data represent dry gas.

Table 1
Data for the combustion engine.

Parameters	Value
Power, KM (kW)	33.5 (24.6)
Vol. displacement, cm^3	3620
Rev. per min	1500
Production year	1971

The temperature changes in the internal reactor (Fig. 7), the changes in the gas components and the contribution of the process gas components during the same period are illustrated in Fig. 8 and agree with the results in Fig. 1.

Figs. 7 and 8 show the progress obtained during the gasification tests for a central pipe height of 190 mm (nominal value; see Fig. 1). A greater periodic variation of the gas deposits caused by a specified fuel dosage to the reactor is noticeable, as is a brief rise in the pressure of the main internal generator. Fig. 7 shows lesser fluctuations observed during the 6 h of operation, illustrating that this behavior is a normal phenomenon for such a system. A similar situation can be observed in the chart in Fig. 8.

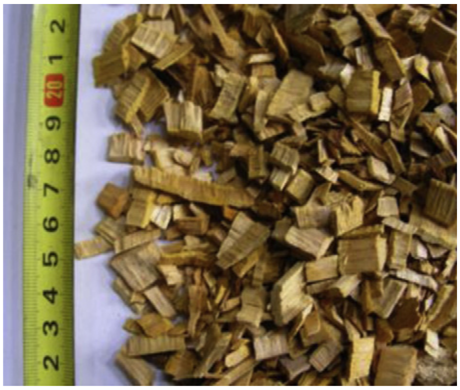

Fig. 6. Image of the studied biomass.

Table 2
Properties of biomass used for gasification.

Denotation	Unit	Chips II
Moisture content	%	14.6
Ash content	%	0.5
Volatile matter content	%	78.97
Sulfur content	%	0.02
Carbon content	%	48.5
Hydrogen content	%	5.75
Nitrogen content	%	0.19
Oxygen content	%	40.15
Higher heating value	J/g	19,084
Lower heating value	J/g	15,654

During the test, a stream of dry air was processed and directed to particular zones in the system, with a summary average value equal to 21.6 Nm^3/h. The dimensions chosen during the research generally provided efficient reactor operation and the appropriate temperature ranges in the specific zones of the process.

This research investigated how changes in the height H_r (changes in the height of the central pipe in relation to the grate surface) influenced the collected gas to verify that the gas collection points were optimal. Fig. 9 shows the process of the solidification changes in the main gas components for a height H_r of 240 mm.

The lower heating value of the combustible gas at a height of $H_r = 240$ mm was 4.40 MJ/Nm^3, which is nominally less than the value obtained for H_r at 190 mm. The gas had similar values for the measured components for both tests, with small deviations only for H_2 and CH_4. There was no noticeable change in the contribution of the main components of the process gas despite shifting the gas collection location 50 mm closer to the pyrolysis zone, and, notably, the products output from the pyrolysis process remained the same (e.g., CH_4). The average values of the process gas deposits obtained from the first and second tests were similar.

Next, tests were conducted with a reduced value of H_r. Fig. 10 shows the changes in the gas composition with time at a height of $H_r = 140$ mm during a 6-h period, including the nominal arrangement of the specific air streams directed to the generator.

Reducing the height to $H_r = 50$ mm significantly changed the composition of the process gas compared to that at the nominal value. Transferring the gas collection point nearer to the combustion zone decreased the value of carbon monoxide from 25.0% to 13.3% and increased the solidification of carbon dioxide from 9.5% to 16.2%. The remaining values of the gas components (i.e., H_2, CH_4 and O_2) do not agree with values from the characteristic test of the nominal parameters. The results are compared in Table 3.

New piston engines require the purity of gas fed to the engine to have no more than 5 mg/Nm^3 ash impurities and 50 mg/Nm^3 organic impurities [8]. Older models had a much higher tolerance for fuel impurities. Therefore, the remaining amount of ash and organic impurities in the reactor was monitored during this study.

Achieving the permissible value of impurities in the residual gas from biomass gasification is a complicated task because of the amount of impurities left and the cost, both in the initial investment and in the installation of the gas purification equipment. A particularly important and troublesome issue is the primary reduction of organic substances. Currently, numerous studies are underway to develop an effective method to reduce organic contaminants with low operational expenditures. Such research activities, among others, are described in detail in prior studies [36,37].

Therefore, the main prerequisite for the dry IOG design at The Institute For Chemical Processing Of Coal in Zabrze was to create an installation that was simple and could be realized with a low financial input compared to its output. The main goal was to reduce ash impurities to below 100 mg/Nm^3 for the dry IOG. The organic impurities were assumed to be mostly consumed in the engine, which should not cause problems if using a current-generating unit (Table 3). We have demonstrated an acceptable solution above, bearing in mind that this gas could be used in an older engine construction that does not require such high fuel purity at the cost of lessened efficiency. Furthermore, these designs are significantly cheaper than those offered by the producers of high-efficiency piston engines.

We achieved the following average efficiencies using the latest configuration of the IOG (consisting of a pressure-reducing valve, a cyclone dust-collector, a gas cooler, a coke adsorber and a cloth filter):

- *Ash impurities*: approximately 95% (from 1500 mg/Nm^3 to 70 mg/Nm^3),
- *Organic impurities*: approximately 47% (from 3600 mg/Nm^3 to 1900 mg/Nm^3).

The stream of ash impurities $\dot{m}_{ash}$ was 70 mg/Nm^3, and the stream of organic impurities $\dot{m}_{tar}$ was 1900 mg/Nm^3.

The average value of the gas purification process is calculated from the average impurities obtained during several tests of biomass gasification.

The final result reduced both the ash and organic impurities to a level at which the gas could be tested in a two-stroke piston engine.

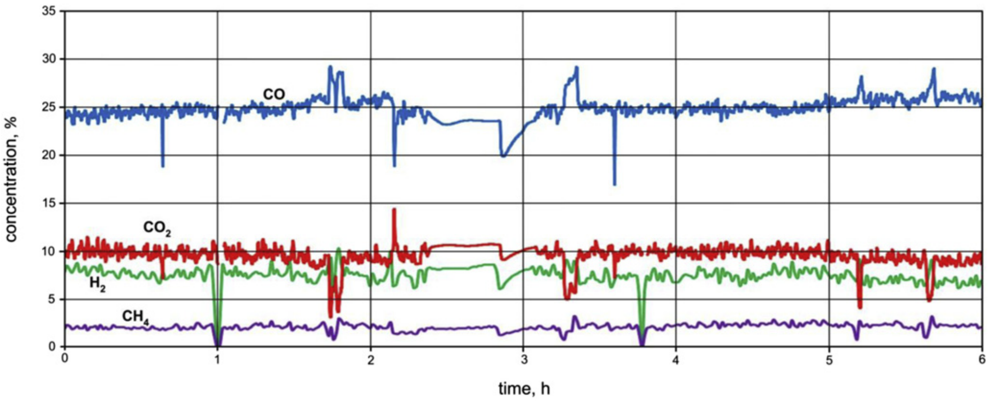

Fig. 7. Changes in the main fuel components during the gasification process: $H_r = 190$ mm.

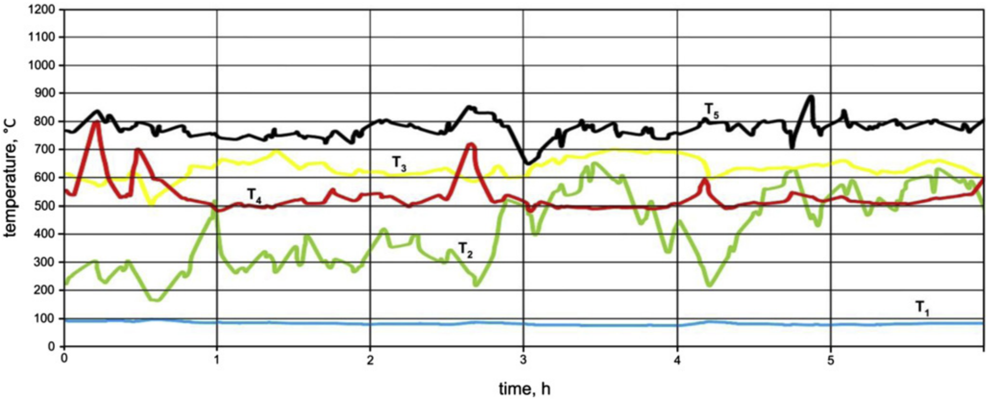

Fig. 8. Changes in the reactor temperature with time: $H_r = 190$ mm.

4.1. Balance of the GG

Measuring the stream of generated gas in the generator was a difficult task [38], mainly because of the relationship between the low governing pressure in the installation and a large amount of ash and organic impurities in the product. This situation caused the impulse conductors to become obstructed and the Prandtl tubes to distort or become totally disabled and thus affected the calculation of the measured value. Hence, we decided to use an estimated balance method to calculate the gas stream $\dot{m}_{gas}$.

An algorithm shown below was used to calculate the generated stream of dry gas and the moisture contained within it for the balance of the GazEla GG.

The applied intermediate method for calculating the value of the gas stream depends on comparing the substratum and the entering products with those exiting from the GG. The concept behind this method is shown in Fig. 11.

The entry data on the entrance side of the generator are shown from the laboratory analysis results of the fuel (Table 2), the average stream of biomass and the average stream of (moist) air measured during the gasification tests for the nominal parameter ($H_r = 190$ mm). On the exit side (product side) of the generator, the balance data consisted of the dry gas composition (CO, CO_2, O_2, H_2, CH_4 and N_2 as a supplement up to 100%; see Table 3) and the stream of organic substances and ash impurities generated during the gasification process. The value of the dry gas stream is denoted as $\dot{m}_{gas\ dry}$, and the value of the moisture stream in the process gas is denoted as $\dot{m}_{H_2O}$. The total estimate of the generated gas stream in the generator is denoted as $\dot{m}_{gas}$.

This calculation method for the balance depends on the assumption of the sought dimensions ($\dot{m}_{gas\ dry}, \dot{m}_{H_2O}$), the subsequent calculation for the stream and all elements (O_2, H_2, C, N_2, S_2) as well as ash (A) ($\dot{m}_{O_2}, \dot{m}_{H_2}, \dot{m}_C, \dot{m}_{N_2}, \dot{m}_{S_2}, \dot{m}_A$) and the sum of these streams (Σm) on both the entry and exit sides of the analyzed fixture. The next stage of the algorithm involves estimating an error margin for the highlighted stream mass for particular components $\delta_i (i = (\dot{m}_{O_2}, \dot{m}_{H_2}, \dot{m}_C, \dot{m}_{N_2}, \dot{m}_{S_2}, \dot{m}_A))$ and their total $\delta_{\Sigma m}$. In this step, a relative error margin was obtained, designated with the assistance of (1) and comparable with the assumed acceptable error margin, which was chosen in this work as 5%.

$$\begin{aligned} \delta_i &= \frac{(\dot{m}_i)_{in} - (\dot{m}_i)_{out}}{(\dot{m}_i)_{in}} \cdot 100\% \\ \delta_{\sum m} &= \frac{\sum_i (\dot{m}_i)_{in} - \sum_i (\dot{m}_i)_{out}}{\sum_i (\dot{m}_i)_{in}} \cdot 100\% \end{aligned} \tag{1}$$

where: δ_i – relative error margin for all elements $i = $ (C, H_2, N_2, O_2, S, A) and their total Σm, $(\dot{m}_i)_{in}$ – stream entering the generator $(\dot{m}_i)_{out}$ – stream exiting the generator.

The next step in the case in which the error margins δ_i or $\delta_{\Sigma m}$ were exceeded (beyond the accepted allowable threshold) was to correct the calculation uncertainties with the assistance of changes in the streams $\dot{m}_{gas\ dry}$ and $\dot{m}_{H_2O}$. The final procedure for the balance took place after fulfilling the condition

$$\delta_i \wedge \delta_{\Sigma m} \leq 5\% \tag{2}$$

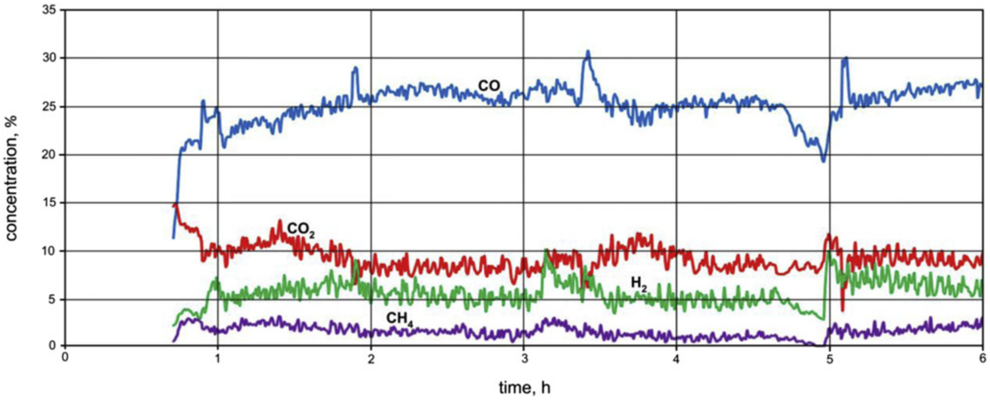

Fig. 9. Process of solidification changes in the main components of the process gas: $H_r = 240$ mm.

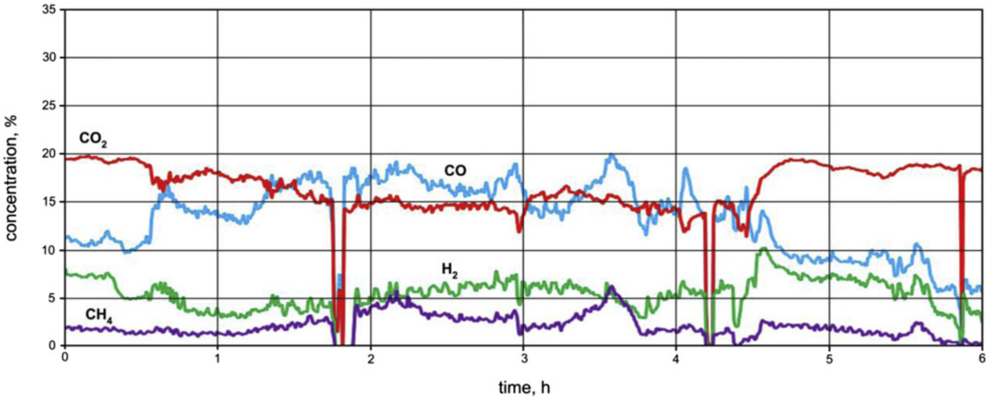

Fig. 10. Changes in solidification of the main components in the process gas: $H_r = 140$ mm.

In Fig. 12, a darker color marks the area that shows the series of solutions for the streams $\dot m_{gas\,s}$ and $\dot m_{H_2O}$ for which it is possible to maintain the maximum error for every element δ_i and their total $\delta_{\Sigma m}$ at a level below 5% (the broken line designates the solution shown in Table 4). A lighter color designates the solution area for errors above 10%. Fig. 13 shows the sample error δ_{O_2} in the functions $\dot m_{gas\,dry}$ and $\dot m_{H_2O}$.

Table 4 shows the results of the accepted GG balancing process for further calculations. The relative errors of all balanced streams are below 5%.

The dry gas stream $\dot m_{gas\,dry} = 36.20$ kg/h, and the moisture contained in the process gas $\dot m_{H_2O} = 6.25$ kg/h based on the estimated balance of the calculated elements. These values allow for the calculation of the contributions on a gram-molecular basis in the moist gas

$$(i) = \frac{[i]}{1 + \frac{\dot m_{H_2O}}{\dot m_{gas\,dry}} \cdot \frac{M_{gas\,dry}}{M_{H_2O}}} \tag{3}$$

where: $i = (H_2O, CO, CO_2, CH_4, H_2, O_2, N_2)$ (data from Table 3) M – particle mass

The results of the calculation are shown in Table 5.

A Sankey diagram for the GazEla GG is plotted in Fig. 14, based on the mass balance data from Table 4. Fig. 15 shows a Sankey diagram with the energy balance for the process GG.

Fuel is fed into the generator at the entrance; this fuel represents nearly the entire stream of energy. Additionally, a small amount of energy is delivered at a low level with the assistance of warmed process air. On the exit side of the reactor, the largest energy stream is contained in the process gas. The result is that the reactor operates at a high gas temperature, which is acceptable, with the average temperature of the gas calculated at the exit of the reactor for Test I and its consumption value (Table 3).

Table 3
Changes in the gas composition and the lower heating value in relation to the height, H_r.

Gas component	Unit	$H_r = 140$ mm (Test III)	$H_r = 190$ mm (Test I)	$H_r = 240$ mm (Test II)
H_2	% vol.	5.4	7.5	5.7
CH_4	% vol.	2.1	2.1	1.7
CO	% vol.	13.3	25.0	25.2
CO_2	% vol.	16.2	9.5	9.3
O_2	% vol.	0.0	0.0	0.0
N_2	% vol.	63.0	55.9	58.1
LHV	MJ/Nm^3	3.01	4.72	4.40

The cold efficiency of the GG, which highlights the relationship between the chemical energy stream contained in the processed gas and the chemical energy stream fed from the biomass to the reactor, may be calculated as follows:

$$\eta_{GG} = \frac{E_{ch\,gas}}{E_{ch\,f}} = \frac{\dot m_{gas} \cdot W_{d\,f}}{\dot m_{pal} \cdot W_{d\,f}} \tag{4}$$

where: η_{GG} – efficiency of the GG (cold).

The η_{GG} value (as calculated based on the data in Tables 2, 4 and 5 and dependent on Eq. (4)) was 62.83% (~63%).

A set of averaged parameters acquired from examples taken during the 6-h-long installation test was used to determine the cold efficiency of the GG.

The hot efficiency η is defined using Eq. (5).

$$\eta = \frac{E_{ch\,gas} + E_{f\,gas}}{E_{ch\,f}} = \frac{\dot m_{gas}\left(W_{d\,gas} + h_{gas}\right)}{\dot m_{fl} \cdot W_{d\,f}} \tag{5}$$

Assuming a gas temperature at the outlet of the reactor of 590 °C (in agreement with Test I), the hot efficiency of the experimental GG was 77.21%. Importantly, the loss to its surroundings is quite large (~20.9%) and is caused by a lack of sufficient thermal isolation of the reactor.

4.2. Research on the biomass gasification system integrated with a SG

The generated process gas combustion tests were conducted in a two-stroke piston engine to study the biomass gasification installation with a GazEla generator. The amount of electrical power generated was controlled using a current-generating unit and a power collection system consisting of electric heaters cooled by an air stream produced by a radial fan. The number of connected heaters determined the current-generating unit load during the research process, producing a variation of 15 kW$_{el}$ in the system work.

The electrical power created in the current-generating unit N_{el} and the stream of (diesel) fuel used, $\dot m_{diesel}$, were measured during the combustion tests. The lower heating value and the density of the diesel fuel were supplied by the fuel producer as $LHV_{diesel} = 43$ MJ/kg and $\rho = 0.84$ kg/dm^3, respectively. The engine fuels used were diesel and the gas from the GG.

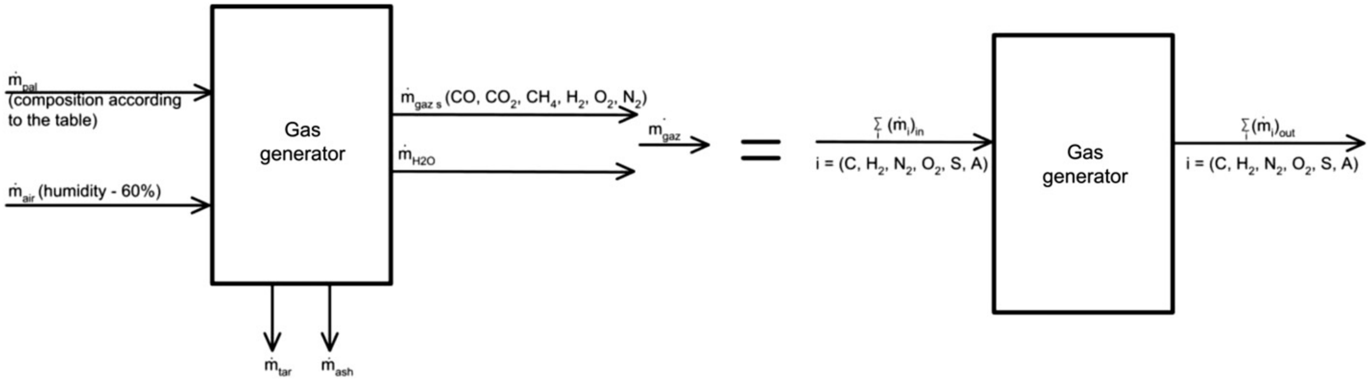
ṁpal
(composition according to the table)
ṁair (humidity - 60%)
Gas generator
ṁgaz s (CO, CO2, CH4, H2, O2, N2)
ṁH2O
ṁgaz
ṁtar
ṁash
=
Σ(ṁi)in
i = (C, H2, N2, O2, S, A)
Gas generator
Σ(ṁi)out
i = (C, H2, N2, O2, S, A)

Fig. 11. Outline of the intermediate calculation method for the process gas stream.

The moist stream of process gas resulted in an estimated balance of elements for the gasification tests of alder chips ($H_r = 190$ mm).

For an engine powered by process gas or diesel fuel, the electrical energy efficiency is defined as

$$\eta_{\mathrm{el}} = \frac{N_{\mathrm{el}}}{\dot{m}_{\mathrm{gas}} \cdot \mathrm{LHV}_{\mathrm{gas}} + \dot{m}_{\mathrm{diesel}} \cdot \mathrm{LHV}_{\mathrm{diesel}}} \tag{6}$$

The combustion of the process gas in a two-stroke piston engine was tested with a variant of the engine using diesel fuel and process gas at a power output of 15.5 $\mathrm{kW_{el}}$.

Diesel fuel was supplied at a rate of 2.4 l/h for an engine working at an electrical power of 15.5 $\mathrm{kW_{el}}$. Furthermore, using the data from Table 5 ($\dot{m}_{\mathrm{gas}}$ and $\mathrm{LHV_{gas}}$), the calculated efficiency of the generated electrical energy in this case was 24.61%. The engine consumed 61.8% process gas and 38.2% diesel oil while generating electrical energy (equal to 15.5 kW_e).

5. Parametric analysis

The following research was conducted on an installation with a power of approximately 60 kW_t. However, in the near future, a new demonstration installation for biomass gasification should be built that includes a GG with a power of 1.5 MW_t (fuel-powered). Additionally, we have constructed a parametric model of a gasification installation with a SG, as shown below. Using this model and the data from the researched installation with a power of 60 kW_t, we were able to designate the efficiency of the installation with a power of 1.5 MW_t and show how several parameters affect the efficiency.

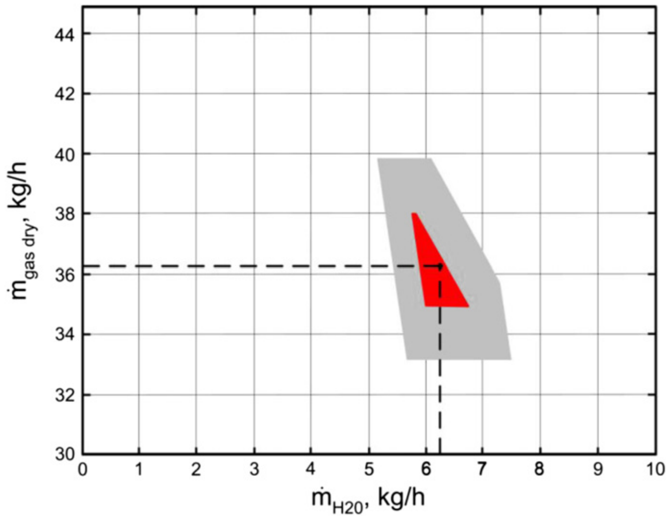

Fig. 12. Common area for errors below 5% (in red) and 10% (in grey) of all components of the balance δ_i and $\delta_{\Sigma m}$.(For interpretation of the references to colour in this figure legend, the reader is referred to the web version of this article.)

The analysis of the accepted model is based on the information presented in Fig. 16, which shows a schematic of the experimental installation [39] that represents the concept of a biomass gasification system integrated with electrical and heat energy generation.

Fig. 16 presents a system consisting of a GG and a ICH (gas-cooling installation) that operates with the assistance of a gas cooler and a IOG, which includes a coke filter and a cloth filter. The purified gas is directed to the SG, where electricity N_{el} and heat energy $\dot{Q}_{23}$ are co-generated. These values were obtained via the cooled process gas in the installation of the cooled gas heat stream $\dot{Q}_{34}$ (the heated stream of the process air) directed to the GG. The remaining part of the collected process heat gas ($\dot{Q}_{35}$) is directed to the mixing chamber KM, where, after joining with the heat stream from the SG, it becomes the heat stream $\dot{Q}_{24}$, which is then fed out of the system. We describe the gross energetic efficiency of this co-generation system as the ratio of the total energy generated in the engine from electrical power N_{el} and the total of the heat streams fed out of the system to the chemical energy of the biomass fed into the reactor, which is consistent with the following equation:

$$\eta_{\mathrm{BCHP}} = \frac{N_{\mathrm{el}} + \dot{Q}_{21} + \dot{Q}_{24}}{(\dot{m} \cdot \mathrm{LHV})_{02}} \tag{7}$$

The energetic efficiency of the process GG (i.e., cold efficiency) may be shown as the ratio of the chemical energy of the process GG $(\dot{m} \cdot \mathrm{LHV})_{11}$ to the chemical energy of the biomass $(\dot{m} \cdot \mathrm{LHV})_{02}$

$$\eta_{\mathrm{GG}} = \frac{(\dot{m} \cdot \mathrm{LHV})_{11}}{(\dot{m} \cdot \mathrm{LHV})_{02}} \tag{8}$$

The efficiencies of the electrical energy generation and the heat generation used for the engine are defined as follows:

$$\eta_{\mathrm{elSG}} = \frac{N_{\mathrm{el}}}{(\dot{m} \cdot W_d)_{15}}, \tag{9}$$

$$\eta_{\mathrm{hSG}} = \frac{\dot{Q}_{23}}{(\dot{m} \cdot \mathrm{LHV})_{15}}. \tag{10}$$

The coefficient of the distribution of gas α is also introduced

Table 4
Element balance for the GazEla gas generator.

	Factor		Streams, kg/h C	H_2	N_2	O_2	S	A	$\Sigma \boldsymbol{m}_i$
Entry	Processed air, m_{air}	Dry air	–	–	20.821	6.290	–	–	27.111
		Air moisture	–	0.088	–	0.700	–	–	0.788
	Biomass moisture, m_{fuel}		5.910	0.932	0.023	7.267	–	0.060	14.200
	Total, $(m_i)_{in}$		5.910	1.020	20.845	14.257	–	0.060	42.099
Exit	Moist gas, m_{gas}	Dry gas,	5.822	0.312	20.845	9.324	–	–	36.199
		Moisture in the gas	–	0.699	–	5.550	–	–	6.250
	Ash, m_{ash}		–	–	–	–	–	0.018	0.018
	Organic substances, m_{tar}		–	–	–	–	–	–	0.190
	Total, $(m_i)_{out}$		5.822	1.011	20.845	14.874	–	0.018	42.657
Relative error, δ%			δ_C	δ_{H_2}	δ_{N_2}	δ_{O_2}	δ_S	δ_A	$\delta_{\Sigma m}$
			1.49	0.88	0.00	−4.33	-[a]	-[b]	−1.32

[a] Not able to be calculated due to a small quantity of sulfur in the researched biomass; the stream value of the balance was not taken into account.

[b] Not able to be calculated due the inability to reliably calculate the value of the ash stream during the experiment. This inability was due to the difficulty in conducting a viable experimental calculation of the ash stream value collected from the bed under the grate of the gas generator. The balance on the exit side includes only the ash coming out of the reactor with the process gas. It is important to emphasize that the value (regardless of position "A") in the mass balance of the reactor was barely 0.1%.

$$\alpha = \frac{\dot{m}_{14}}{\dot{m}_{13}}. \tag{11}$$

The system requirements for the process gas (e.g., the amount of gas necessary to generate an appropriate combustion stream in the combustion chamber to dry the biomass, defined in Eq. (11)) and the efficiency of the generated electrical energy and the efficiency of the generated heat in the piston engine (defined as dependent on Eqs. (9) and (10)) may be written as

$$\eta_{elSG} = \frac{N_{el}}{(1-\dot{\alpha})\cdot(\dot{m}\cdot \mathrm{LHV})_{13}}, \tag{12}$$

$$\eta_{hSG} = \frac{\dot{Q}_{23}}{(1-\alpha)\cdot(\dot{m}\cdot \mathrm{LHV})_{13}}. \tag{13}$$

In the analysis of this case, the heat stream $\dot{Q}_{21}$ may be designated as

$$\dot{Q}_{21} = \dot{Q}_{16} + \alpha\cdot(\dot{m}\cdot \mathrm{LHV})_{13}. \tag{14}$$

Introducing the energetic efficiency of the IOG in relation to the chemical gas energy before and after the purification process yields

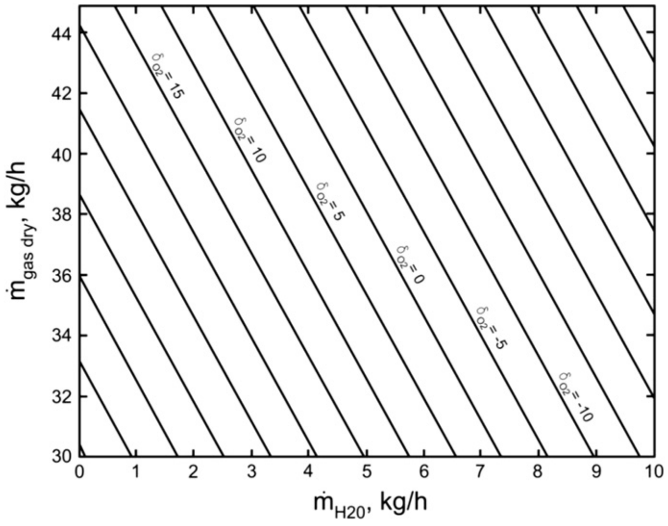

Fig. 13. Permanent line of error margin δ_{O_2} for the moisture stream $\dot{m}_{H_2O}$ and the dry gas stream $\dot{m}_{gas\ dry}$ functions.

$$\eta_{IOG} = \frac{(\dot{m}\cdot \mathrm{LHV})_{13}}{(\dot{m}\cdot \mathrm{LHV})_{12}}. \tag{15}$$

We record the thermal power $\dot{Q}_{21}$ in the form of

$$\dot{Q}_{21} = \dot{Q}_{16} + \eta_{IOG}\cdot\alpha\cdot(\dot{m}\cdot \mathrm{LHV})_{12}. \tag{16}$$

Additionally, the heat power $\dot{Q}_{24}$ is designated as

$$\dot{Q}_{24} = \eta_1\cdot\dot{Q}_{23} + \eta_2\cdot\dot{Q}_{35}. \tag{17}$$

The adiabatic balance of the process ICH (gas-cooling system) and the IOG (gas purification installation) (omitting the heat content of a gasifying agent) at a given temperature setting may be written as

$$\dot{Q}_{35} + \dot{Q}_{16} + \dot{Q}_{34} = \dot{m}_{11}\cdot(h_{13} - h_{11}). \tag{18}$$

Making use of the dependencies described earlier and introducing the additional parameters in agreement with the following equations gives:

$$\begin{aligned} u_1 &= \frac{h_{11}}{\mathrm{LHV}_{11}}, u_2 = \frac{h_{12}}{\mathrm{LHV}_{12}}, \\ w &= \frac{\dot{Q}_{16}+\dot{Q}_{34}}{\dot{Q}_{35}}, w_1 = \frac{\dot{Q}_{16}}{\dot{Q}_{35}}. \end{aligned} \tag{19}$$

The general efficiency of the biomass gasification system for electrical and heat energy generation may be written as follows:

$$\begin{aligned} \eta_{BCHP} = \eta_{GG}\cdot\eta_{IOG}\Bigg[&(1-\alpha)(\eta_{elSG}+\eta_{hSG}\cdot\eta_1) \\ &+ \frac{(u_1-u_2)}{(1+w)\eta_{IOG}}(w_1+\eta_2)+\alpha\Bigg]. \end{aligned} \tag{20}$$

Table 5
Values of the main components of damp gas.

Gas component	Unit	Value
H_2	% vol.	5.9
CH_4	% vol.	1.7
CO	% vol.	19.8
CO_2	% vol.	7.5
O_2	% vol.	0.0
H_2O	% vol.	20.8
N_2	% vol.	44.3
LHV_{gas}	MJ/Nm^3	3.74
m_{gas}	kg/h	42.45

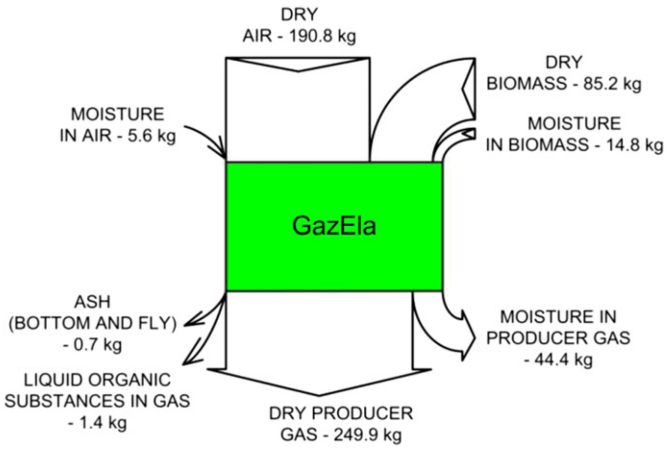

Fig. 14. Mass balance for biomass gasification in a GazEla generator (for 100 kg of fuel under working conditions).

Setting $\alpha = 0$ and obtaining $w_1 = 0$, the entire stream of the process gas from the generator is directed to the SG, and the overall efficiency of the system is expressed as

$$\eta_{\mathrm{BCHP}} = \eta_{\mathrm{GG}} \cdot \eta_{\mathrm{IOG}} \left[(\eta_{\mathrm{elSG}} + \eta_{\mathrm{hSG}} \cdot \eta_1) + \frac{(u_1 - u_2)}{(1+w)\eta_{\mathrm{IOG}}} \cdot \eta_2 \right]. \tag{21}$$

Eqs. (20) and (21) presented above show the influence of the efficiency of specific unit processes on the energetic efficiency of the entire installation. In the above equations, we accept that $\mathrm{LHV}_{13} = \mathrm{LHV}_{14} = \mathrm{LHV}_{15}$.

Table 6 presents the assumptions for an installation with a power of 1.5 MW_t. The basic presuppositions are as follows:

1. The gas composition and the combustion value in the GG are assumed to be the same as those in the researched system (Test I).
2. The GG is assumed to have the same cold efficiency as that in the researched system ($\eta_{\mathrm{GG}} = 63\%$).
3. The energy loss to the surroundings in the GG is limited to 10% from a value of 20.87% and an increase in the exiting gas temperature (i.e., at point 11 in Fig. 16) and the consequent coefficient growth u_1. The increase in the temperature of the exiting gas in relation to the measured value is confirmed in the calculated models conducted with the Aspen Plus program. The accepted temperature of the gas at point 11 (Fig. 16) is 950 °C.
4. The efficiency of the electrical energy generation in the SG η_{elSG} is assumed to be 36.2% (i.e., significantly higher than that in the researched engine at 24.6%) on the basis of Ref. [8].
5. The efficiency of heat generated η_{hSG} in the SG is assumed to be 40.2%; such an efficiency level does not include the use of low-temperature heat, which could increase the efficiency by up to 8%.
6. Part of the heat transferred through the process gas in the ICH is assumed to be directed back to the generator (stream $\dot{Q}_{34}$) with the assistance of the heated process air at a temperature of 200 °C. Moreover, the increase in the temperature of process air from 30 °C to 200 °C only influences the increase in the temperature of the gas at the exit of the generator, and the change of this parameter does not cause a change in the composition of the process gas.

Using the accepted data, a sensitivity analysis was performed, and the results are shown in Fig. 17. The results show how particular compositions of the model influence (21) (in the range of their values from −0.03 to 0.03) the efficiency of the GG (η_{GG}), the efficiency of the electric energy generation in the engine (η_{elSG}), the efficiency of the heat generation in the electrical engine (η_{hSG}), the efficiency of η_1 and η_2, the efficiency of the IOG (η_{IOG}) and show the effect of the coefficients u_1, u_2 and w on the efficiency of the overall system η_{BCHP}, among others. The influence of the efficiency changes in the individual units and the analyzed coefficients on the efficiency of the entire system is linearly dependent. The change in specific starting compositions in the composition model of Eq. (21) shows relatively similar behavior.

The conducted parametric analysis of the biomass gasification installation integrated with a SG shows how specific elements of the installation affect the efficiency of the entire biomass gasification installation η_{BCHP}. The greatest influence on the system efficiency η_{BCHP} is that of the GG η_{GG}. For a nominal level of generator efficiency (63.0%), the system efficiency rose to 71.9%. When the reactor efficiency decreased to 60.0%, the efficiency of the gasification installation also decreased to 68.5%. However, when the reactor efficiency increased to 66.0%, the installation efficiency increased to 75.3%. The second vital parameter influencing the η_{BCHP} is the electrical energy generation efficiency in the SG. Increasing or decreasing this value by 0.03 causes the system's efficiency to shift from 70.1% to 73.7%. The heat generation efficiency

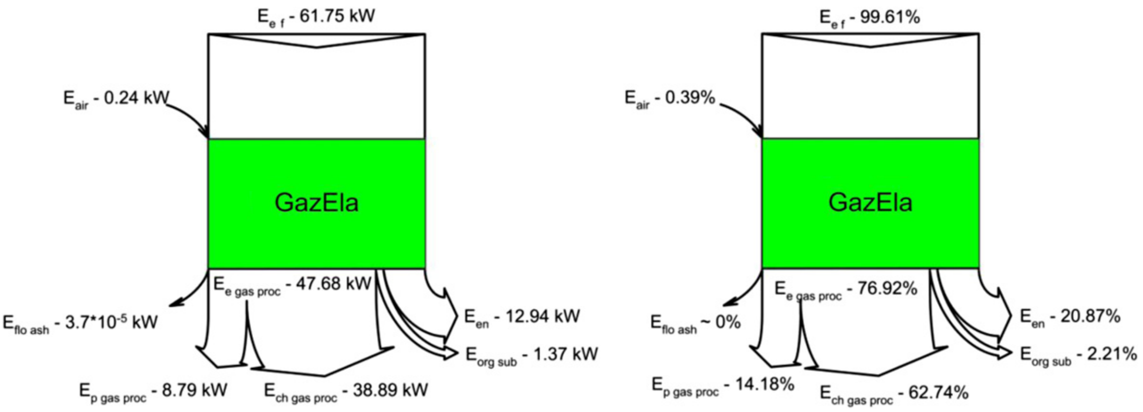

Fig. 15. Energy balance for biomass gasification of the tested GazEla generator (index: f – fuel, air – process air, gas proc – process gas, org sub – organic substances, flo ash – floating ash, en – environment, p – physical, ch – chemical, e – entire).

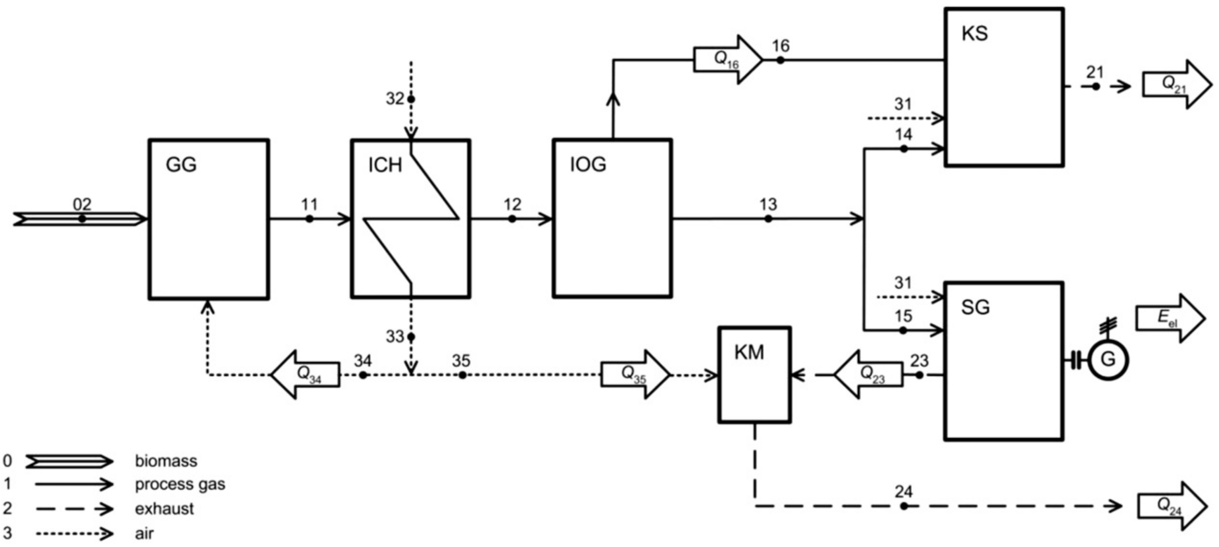

Fig. 16. Block outline of a biomass gasification installation with a gas generator and a power of 1.5 MW$_t$.

Table 6
Assumptions for the parametric analysis of the biomass gasification system at a power of 1.5 MW$_t$.

Designation	Symbol	Unit	Value
Gas stream	$\dot{m}_{11}$	kg/h	1031.5
Value of the combusted gas	LHV_{11}	kJ/kg	3300
Temperature of the gas at point 11	t_{11}	°C	950
Temperature of the gas at point 13	t_{13}	°C	40
Heat stream at point 35	$\dot{Q}_{35}$	kW	360
Heat stream at point 34	$\dot{Q}_{34}$	kW	38
Efficiency of the gas generator when cold	η_{GG}	%	63
Efficiency of electrical energy generation in the engine	η_{elSG}	%	36.2
Efficiency of heat generation in the engine	η_{hSG}	%	48.2
Efficiency of the gas purification system	η_{IOG}	%	97
Efficiency of heat transformation	η_1	%	97
Efficiency of heat transformation	η_2	%	97
Coefficient of the distribution of gas	α	–	0
Coefficient	u_1	–	0.39
Coefficient	w	–	0.105

in the SG chamber similarly affects the efficiency of the biomass gasification system in the range of 70.1–73.7%.

6. Discussion and conclusions

The process of generating electrical and heat energy will soon be connected with decision-making and intensive work aimed at lowering the harmful environmental effects of the energy industry. One interesting direction that may improve the eco-friendliness of energy generation is the use of RES, such as biomass. The specific properties of biomass and the potential for its use make it a particularly desirable solution for fuel in the context of gasification technology. Converting the chemical energy contained in the biomass to combustible gas energy enlarges the energetic sphere for the use of biomass. Using process gas as a fuel for dispersed small- and average-sized electrical energy and heat co-generation systems may allow Poland and the EU to achieve the target minimal value for RES in the overall fuel use. Furthermore, these systems encourage the use of local fuel sources, thus eliminating transport costs. These systems also have the advantage of leveraging fuel sources that are often regarded as waste products (e.g., from the timber or food industries).

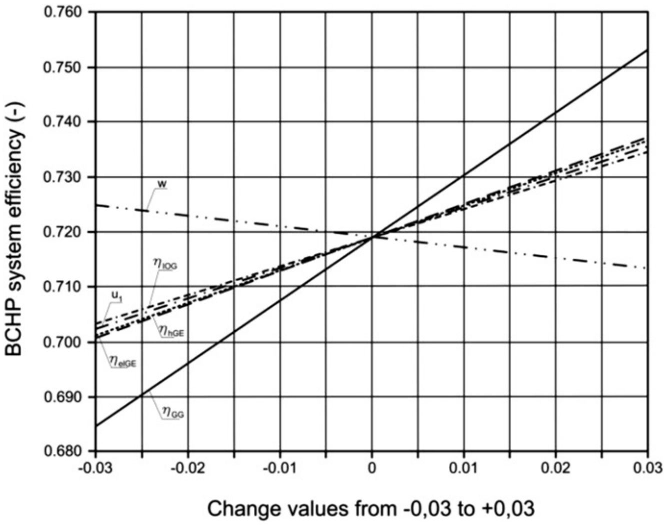

Fig. 17. Influence of the efficiency of the gas generator (η_{GG}), the efficiency of the electrical energy generation in the gas engine (η_{elSG}), the efficiency of heat generation within the engine (η_{hSG}), the efficiencies η_1 and η_2, the efficiency of the gas purification system (η_{IOG}) and the effects of coefficients w, u_1 and u_2 of the efficiency of the entire system (η_{BCHP}).

During the development of the research installation in IChPW, a series of tests was conducted over many hours with the aim of controlling the function of the entire installation, with particular attention paid to the GG. An important value was the set-up of the construction parameters and, most importantly, the appropriate height of H_r, the distance between the air distributor and the gas outlet to the central pipe. Tests conducted at various heights showed how the height influenced the maximum combustion value of the generated gas. The collected results in Table 3 show the influence of the height H_r on the composition and combustion value of the process gas. For the three values of height H_r presented, the lowest heating values of the gas occurring in the chamber ranged from 3.02 MJ/Nm^3 to 4.72 MJ/Nm^3. The greatest gas heating values were obtained for a height of H_r = 190 mm, which was used as nominal in the subsequent studies.

One of the important points realized in the course of this research was the impact of the amount of moisture contained in the generated gas stream. Due to difficulties connected with the direct measurement of these values, a portion of the researched methodology focused on this stream of moist gas. An average balance method was found to be acceptable depending on the assumption of a dry gas stream and a moist air stream. Testing was conducted to search for two values for which the maximum error margin of all elements entering and exiting the generator was less than 5%, the allowable value for the designation sought. The value of the stream of moist gas (for Test I) was 42.45 kg/h, and the moisture contained in the gas streams was 6.25 kg/h. For the highlighted streams, the compositions of the moist gas were $CO = 19.8\%$, $CO_2 = 7.5\%$, $H_2O = 20.8\%$, $H_2 = 5.9\%$, $CH_4 = 1.7\%$ and $N_2 = 44.3\%$.

In this paper, a Sankey diagram was used to show the mass stream flow and the outflow from the research fixtures (for an estimated 100 kg of fuel) as well as the energetic balance of the gasifier. The cold efficiency in the GG was approximately 62.8%.

The final configuration of the purification system removed approximately 95% of the ash impurities and 47% of the organic impurities.

The purified gas was used as a source of chemical energy in the form of hot fumes in a two-stroke piston engine to generate electrical and heat energy. The stream of the obtained electrical gas during the tests corresponded to 15.5 kW_{el}. The engine used in the research, which used diesel as a basic fuel during the combustion of process gas and liquid fuel, was characterized by a relatively low efficiency in comparison with current commercial solutions. The obtained efficiency for the generated electrical energy at the nominal parameters of the engine work was approximately 24.6%, which was produced using 61.8% process gas, with diesel fuel accounting for the remaining 38.2%.

In this article, we also present a parametric model of a system for generating electrical and heat energy integrated with a GG. Our research shows how a particular composition of system elements influences the overall efficiency of the biomass gasification installation integrated with a commercial gas piston engine using the data obtained from the conducted experimental research and simulating calculations for a system with greater power (i.e., 1.5 MW_t). The greatest influence on the efficiency of the system is the cold efficiency of the GG. In the case in which this efficiency grew from 60% to 66%, the efficiency of the entire system was increased from 68.5% to 75.3%. In contrast, when the cold efficiency of the reactor was 69%, the efficiency of the installation was 78.8%. The obtained results confirm that optimizing the work of both the overall system in this particular GG (through the use of the appropriate prepared fuel) and the work of the reactor, which should be constructed with satisfactory thermal installation, are essential to the system's performance. Possible methods to correct the cold efficiency of the generators include increasing the temperature of air input to the process or feeding this air with condensation or oxygen. In the case of a low- or average-power system, the process may be too costly, and further improvements will be the subject of future analysis and research.

Acknowledgments

The investigations in this paper were performed under research project no. N N513 360537 from 2009 to 2012, which was financed by the Ministry of Education and Science as part of the strategic program of scientific research and experimental development of the National (Polish) Center for Research and Development: “Advanced Technologies for Energy Generation”; Task 4, “Elaboration of Integrated Technologies for the Production of Fuels and Energy from Biomass as well as from Agricultural and other Waste Materials”.

References

[1] Kotowicz J, Bartela Ł. A parallel co-firing of biomass in a supercritical coal fired power plant – Part II. Rynek Energii 2009;1(80):53–8 [in Polish].
[2] Chmielniak T. Energy technologies. Gliwice: Silesian University of Technology Publishing House; 2004 [in Polish].
[3] Ściążko M, Zuwała J. Full-scale co-firing trial tests of sawdust and bio-waste in pulverized coal-fired 230 t/h steam boiler. Biomass and Bioenergy 2010;34: 1165–74.
[4] Ziębik A, Zuwała J, Ściążko M. Energy and ecological effectiveness of biomass co-firing in CHP plant. Archives of Thermodynamics 2009;2:29–44.
[5] Kirkels AF, Verbong GPJ. Biomass gasification: still promising? A 30-year global overview. Renewable and Sustainable Energy Reviews 2011;1:471–81.
[6] Ptasinski KJ, Janssen FJJG. From coal to biomass gasification: comparison of thermodynamic efficiency. Energy 2007;7:1248–59.
[7] Ptasinski KJ. Exergy analysis of bioenergy. In Gasification, biofuels, implications. Eindhoven; 2008.
[8] Chmielniak T, Skorek J, Kalina J, Lepszy S. Integrated power systems with biomass gasification. Gliwice: Wydawnictwo Politechniki Śląskiej; 2008 [in Polish].
[9] Kotowicz J, Sobolewski A, Iluk T, Matuszek K. Biomass gasification in a fixed bed gasifier. Rynek Energii 2009;2(81):52–8 [in Polish].
[10] Juan DM, Electo ESL, Rubenildo VA, René LJ. Experimental study on biomass gasification in a double air stage downdraft reactor. Biomass and Bioenergy 2011;8:3465–80.
[11] Plis P, Wilk KR. Theoretical and experimental investigation of biomass gasification process in a fixed bed gasifier. Energy 2010;36:3838–45.
[12] Gil J, Corella J, Aznar MP, Caballero MA. Biomass gasification in atmospheric and bubbling fluidized bed. Effect of the type of gasifying agent on the product distribution. Biomass and Bioenergy 1999;5:389–403.
[13] Li XT, Grace JR, Lim CJ, Watkinson AP, Chen HP, Kim JR. Biomass gasification in a circulating fluidized bed. Biomass and Bioenergy 2004;2:171–93.
[14] Lv PM, Xiong ZH, Chang J, Wu CZ, Chen Y, Zhu JX. An experimental study on biomass air-steam gasification in a fluidized bed. Bioresource Technology 2004;95:95–101.
[15] Kotowicz J, Iluk T. Integrated gasification combined cycles. Rynek Energii 2008;3(76):34–40 [in Polish].
[16] Schaffel N, Szlęk A. An analysis of the usability of gas in biomass gasification in a Polish heating plant: (Contemporary Heating-Plants). In Nowoczesne Ciepłownictwo: (Contemporary Heating-Plants) 2004. p. 12, [in Polish].
[17] Wilk RK, Plis P. Co-combustion of syngas obtained from air-biomass gasification with coal in small scale boilers. In Environmental Engineering III. London: Taylor & Francis Group; 2010. pp. 591–5.
[18] Kalisz S, Pronobis M, Baxter D. Co-firing of biomass waste derived syngas in coal power boiler. Energy 2008;12:1770–8.
[19] Rapagná S, Provendier H, Petit C, Kiennemann A, Foscolo PU. Development of catalysts suitable for hydrogen or syn-gas production from biomass gasification. Biomass and Bioenergy 2002;5:377–88.
[20] Juraščík M, Sues A, Ptasinski KJ. Exergy analysis of synthetic natural gas production method from biomass. Energy 2010;2:880–8.
[21] Matsumoto K, Takeno K, Ichinose T, Ishii H, Nishimura K. Development of a 2 ton/day-scale test plant for total operation study of woody biomass gasification and liquid fuel synthesis. In: Proceedings of the 15th European biomass conference & exhibition. Germany; 7–10 May 2007.
[22] Chmielniak T, Ściążko M. Co-gasification of biomass and coal for methanol synthesis. Applied Energy 2003;3–4:393–403.
[23] Holmgren KH, Berntsson T, Andersson E, Rydberg T. System aspects of biomass gasification with methanol synthesis – process concepts and energy analysis. Energy 2012;45:817–28.
[24] Klimantos P, Noukouzas N, Katsiadakis A, Kakaras E. Air-blown biomass gasification combined cycles (BGCC): system analysis and economic assessment. Energy 2009;34:708–14.
[25] Prins MJ, Ptasinski KJ, Janssen FJJG. More efficient biomass gasification via torrefaction. Energy 2006;32:3458–70.
[26] Fischer B, Pigneri A. Potential for electrification from biomass gasification in Vanuatu. Energy 2011;36:1640–51.
[27] Chmielniak T, Lepszy S, Wójcik K. Analysis of gas turbine combined heat and power system for carbon capture installation of coal-fired power plant. Energy 2012;45:125–33.
[28] Sobolewski A, Kotowicz J, Iluk T, Matuszek K. Experimental studies on biomass gasification from the point of view of the process gas use in the cogeneration system. Przemysł Chemiczny 2010;6:794–8 [in Polish].
[29] Kotowicz J, Sobolewsk A, Iluk T, Matuszek K. Experimental studies of biomass gasification installation consisting of a new gasifier and gas cleaning system. In: Proceedings of the 23rd international conference ECOS 2010. Lausanne, Switzerland; 14–17th June 2010. p. 583–8.
[30] Sobolewski A, Ilmurzyńska J, Iluk T, Czaplicki A. Biomass gasification in monography. In: Bocian P, Golec T, Rakowski J, editors. Chapter entitled: modern technologies of acquiring and energy utilization of biomass. Warsaw: Publication of the Institute of Energy; 2010. p. 280–309.

[31] http://www.gvepinternational.org/sites/default/files/factsheet_gasifier_web_final.pdf. date of entry 10 September 2012.

[32] Najser J, Ochodek T, Chłond R. Character of operations of the biomass gasification installation and economic aspects of electricity generation. Rynek Energii 2009;6(85):68–74 [in Polish].

[33] http://www.wxhuguang.com. date of entry 10 September 2012.

[34] http://feng-yu.com. date of entry 10 September 2012.

[35] Sobolewski A, Kotowicz J, Iluk T, Matuszek K. The influence of biomass type on the operating parameters of a fixed-bed gasifier. Rynek Energii 2009;3(82):53–8 [in Polish].

[36] Hun J, Kim H. The reduction and control technology of tar during biomass gasification/pyrolysis: an overview. Renewable and Sustainable Energy Reviews 2008;12:397–416.

[37] Devi L, Ptasinski KJ, Janssen FJJG. A review of the primary measures for tar elimination in biomass gasification processes. Biomass and Bioenergy 2003;2:125–40.

[38] Węcel D, Chmielniak T, Kotowicz J. Experimental and numerical investigations of the averaging Pitot tube and analysis of installation effects on the flow coefficient. Flow Measurement and Instrumentation 2008;5:301–6.

[39] Kotowicz J, Iluk T. Installation of biomass gasification integrated with a combustion engine. Rynek Energii 2011;3(94):47–52 [in Polish].